Journal of Medicinal Chemistry

Article

pubs.acs.org/jmc

Rational Design, Synthesis, and Preliminary Structure–Activity Relationships of α-Substituted-2-Phenylcyclopropane Carboxylic Acids as Inhibitors of *Salmonella typhimurium* *O*-Acetylserine Sulfhydrylase

Marco Pieroni,[†,■] Giannamaria Annunziato,[†,■] Claudia Beato,[†] Randy Wouters,[†,¶] Roberto Benoni,[‡] Barbara Campanini,[*,‡] Thelma A. Pertinhez,[§,△] Stefano Bettati,[⊥,∥] Andrea Mozzarelli,[‡,∥,#] and Gabriele Costantino[*,†]

[†]P4T group, [‡]Laboratory of Biochemistry and Molecular Biology, Department of Pharmacy, and [§]Centro Interdipartimentale Misure (CIM)'G. Casnati', University of Parma, Parco Area delle Scienze 27/A, 43124 Parma, Italy

[⊥]Department of Neurosciences, University of Parma, Via Volturno, 39, 43125 Parma, Italy

[∥]National Institute of Biostructures and Biosystems, Viale delle Medaglie d'Oro 305, 00136 Rome, Italy

[#]Institute of Biophysics, CNR, /o Area di Ricerca San Cataldo, Via G. Moruzzi N° 1, 56124 Pisa, Italy

Supporting Information

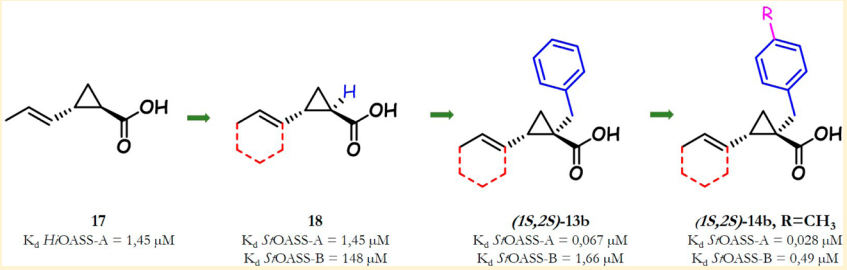

ABSTRACT: Cysteine is a building block for several biomolecules that are crucial for living organisms. The last step of cysteine biosynthesis is catalyzed by *O*-acetylserine sulfydrylase (OASS), a highly conserved pyridoxal 5′-phosphate (PLP)-dependent enzyme, present in different isoforms in bacteria, plants, and nematodes, but absent in mammals. Beside the biosynthesis of cysteine, OASS exerts a series of "moonlighting" activities in bacteria, such as transcriptional regulation, contact-dependent growth inhibition, swarming motility, and induction of antibiotic resistance. Therefore, the discovery of molecules capable of inhibiting OASS would be a valuable tool to unravel how this protein affects the physiology of unicellular organisms. As a continuation of our efforts toward the synthesis of OASS inhibitors, in this work we have used a combination of computational and spectroscopic approaches to rationally design, synthesize, and test a series of substituted 2-phenylcyclopropane carboxylic acids that bind to the two *S. typhymurium* OASS isoforms at nanomolar concentrations.

INTRODUCTION

Cysteine is the amino acid precursor of all sulfur-containing biomolecules, including methionine, CoA, biotin, Fe–S clusters, penicillin, and glutathione, that are vital for the majority of living organisms.[1] Mammals lack the biosynthetic machinery that leads to the *de novo* synthesis of cysteine from inorganic sulfur, whereas bacteria and plants possess redundant and highly conserved enzymes enabling cysteine biosynthesis (Figure 1A). In enteric bacteria the last two steps of cysteine biosynthesis (Figure 1B) are catalyzed by serine acetyltransferase (SAT) and *O*-acetylserine sulfhydrylase (OASS).[2]

The two enzymes form the so-called "cysteine synthase complex" that is stabilized by the interaction of the C-terminal portion of SAT with the substrate binding pocket of OASS. The first identified OASS isoform, named OASS-A, was originally isolated and characterized from *Salmonella typhimu-*

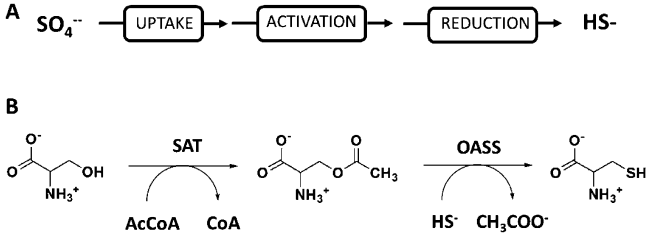

Figure 1. (A) Uptake and reduction of inorganic sulfur by microorganisms. (B) Cysteine biosynthesis from serine.

Received: November 13, 2015

DOI: 10.1021/acs.jmedchem.5b01775
J. Med. Chem. XXXX, XXX, XXX–XXX

rium. Later, it was noticed that many organisms possess two isoforms of the enzyme, that show homology although with peculiar functional and structural properties: *O*-acetylserine sulfhydrylase (OASS-A, encoded by *cysK*)[3] and *O*-phosphoserine sulfhydrylase (OASS-B, encoded by *cysM*). In *S. typhimurium*, both isozymes use *O*-acetylserine as first substrate and bisulfide as sulfur source. In addition to bisulfide, OASS-B can also use thiosulfate. OASS-A and OASS-B are differently expressed under aerobic/anaerobic conditions[2,4] but their specific role is still partly unclear. Both enzymes are pyridoxal 5′-phosphate (PLP)-dependent and share a similar Bi−Bi ping-pong type reaction mechanism. In the first half-reaction, the β-elimination of the β-substituted L-serine external aldimine takes place with the accumulation of the α-aminoacrylate intermediate Schiff base. In the second half-reaction, the α-aminoacrylate is attacked by sulfide or thiosulfate with formation of cysteine.[5] The three-dimensional structures of OASS-A and OASS-B[6−20] invariably show a dimeric assembly with each subunit organized into two domains and the active sites, each carrying a molecule of PLP, facing the solvent (Figure 2A). The two domains are flexible and close upon

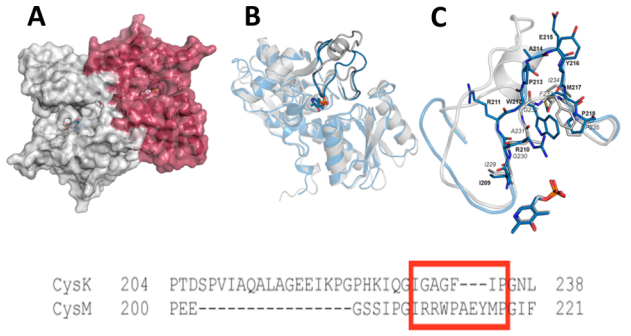

Figure 2. (A) Homodimer of OASS-A taken from 1OAS crystal structure; the two monomers are highlighted with different colors. (B) Superposition of OASS-A (1OAS chain A, in light gray) and OASS-B (2JC3 chain A, in blue). The major structural difference concerning the loops above the binding site is highlighted; the sequences of the loops of the two isoforms, aligned as in the superposition of the two crystal structures, are reported at the bottom of the figure. (C) Zoom on the loops highlighted in panel B: OASS-A in light gray with residues labeled in italics; OASS-B in blue with residues labeled in bold. The structure-based amino acid sequence alignment of the loops of the two isoforms is reported at the bottom of the figure.

substrate binding, thus allowing diffusion into the active site only of small molecules and protecting the highly reactive α-aminoacrylate intermediate from attack by water or other nucleophiles. OASS-A and OASS-B exhibit 40% sequence identity and 56% sequence similarity[21] and a very similar structural fold, belonging to the fold type II family of the PLP-dependent enzymes[22,23] (Figure 2B). However, major differences can be detected in the region of the flexible loop located at the entrance of the active site (Figure 2C). In particular, in the B isoform the motif Gly230-Ala231-Gly232 is replaced by Arg210-Arg211-Trp212 (*S. typhimurium* numbering scheme), increasing the overall polarity and causing a variation in the size of the binding site.

Since its discovery, OASS was thought to be involved only in the biosynthesis of cysteine, but recently a growing number of additional "moonlighting" activities have been identified.[24] Indeed, OASS-A activities span from transcriptional regulation in some bacteria and nematodes[25,26] to toxin activation in *E. coli*,[27] from swarming motility in *Proteus mirabilis*[28] and *S. typhimurium*[29] to antibiotic resistance.[30,31]

Considering the multifaceted functions of this enzyme, and considering that the biosynthesis of cysteine is not shut down unless both enzymes are inhibited,[4] the discovery of molecules that interact with both isoforms of OASS and inhibit their activity would be a valuable tool to investigate the physiological role of these enzymes in unicellular organisms.[32] Since SAT competitively inhibits OASS-A, the structural features of OASS-SAT interaction have paved the way to the rational design of the first sulfhydrylase inhibitors. Starting from the structure of the physiological inhibitor of OASS, Salsi et al. have analyzed at the molecular level the interaction of SAT C-terminal peptide with OASS active site[33] and have studied the kinetics of SAT-OASS complex formation from *Haemophilus influenzae*.[34] These studies supported the view that the last five amino acids of the carboxy-terminal portion of *Hi*SAT (MNLNI) (Figure 3) are

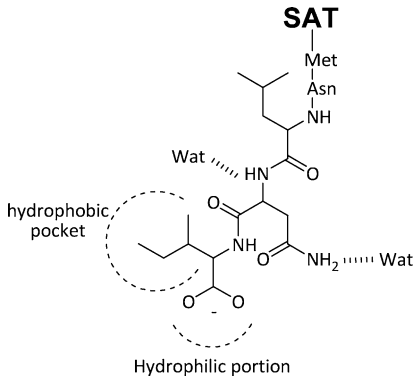

Figure 3. Structure of the carboxy-terminal portion of *Hi*SAT in the active site of *Hi*OASS as inferred from the three-dimensional structure of the complex between *Hi*OASS and the MNLNI peptide.[6]

predominantly responsible for the interaction with OASS, and, in particular, the C-terminal isoleucine is essential for this interaction.[6,33,35] Indeed, although the primary structure of SAT C-terminal peptide is species-specific in bacteria, it invariantly carries a terminal isoleucine.[36]

A previous attempt to identify OASS inhibitors was carried out by exploiting a small library of pentapeptides, leading to the identification of molecules with affinities in the micromolar range.[33,37] In order to circumvent the chemical liabilities of peptides such as low stability and low bioavailability, while maintaining the enzyme inhibition, we carried out an *in silico* campaign[21] and also prepared a number of small molecules inspired by the structures of these peptides.[38] We reasoned that the acid moiety of the isoleucine was crucial for the activity, since it establishes a dense network of hydrogen bonds with the backbone of several residues belonging to the catalytic pocket, namely, Asn72, Thr73, Thr69, and Gln143 (Figure 4).

An alkyl moiety mimicking the side chain of isoleucine was attached to the carboxylic acid moiety through a suitable spacer that could maintain the two anchoring arms of isoleucine into the favorable *trans* configuration. For this purpose, a cyclopropane scaffold was selected. Despite the good affinity toward *Hi*OASS-A, the majority of the prepared compounds suffered from several weaknesses, such as poor chemical feasibility and stability. Therefore, we have initiated a program directed to the design and synthesis of novel substituted cyclopropane-carboxylic acids, aimed at improving their stability and their potency toward both the OASS-A and OASS-B isoforms. The

DOI: 10.1021/acs.jmedchem.5b01775
J. Med. Chem. XXXX, XXX, XXX−XXX

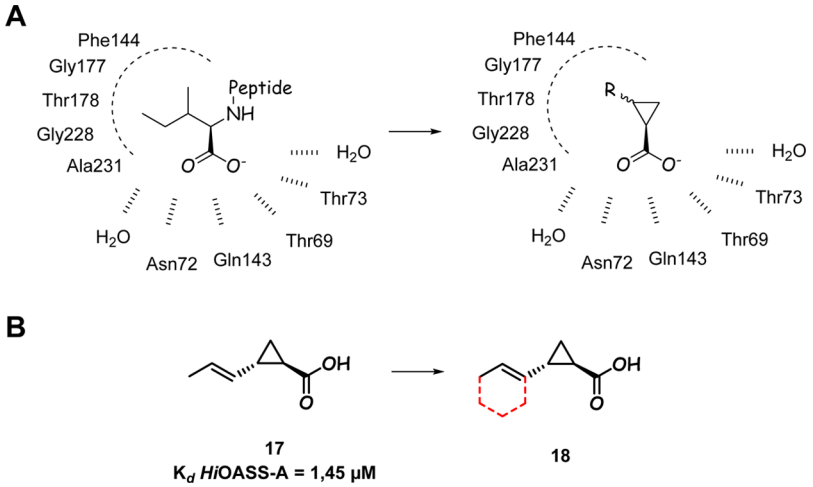

Figure 4. (A) Rational design of cyclopropane carboxylic acids. (B) Expansion of the series from compound **17**.

results are reported herein and, to the best of our knowledge, some of the newly prepared compounds represent the most potent binders of the B isoform reported so far. Furthermore, insights into the mechanism of ligand/protein interaction were obtained with the integration of computational and spectroscopic methods, providing the basis for further chemical optimization of these chemical tools.

CHEMISTRY

The 2-phenylcyclopropane carboxylic acids (**12a−c**, **13a−c**, **14a−c**, **15a−c**, and **16a**) were prepared through a straightforward protocol already reported,[39−41] reacting the appropriate styrene oxides **a−c** with the suitable phosphonates in dimethoxyethane at 130 °C using butyllithium as deprotonating agent. This procedure has the advantage to direct in the *trans* position the carboxylic moiety and the phenyl ring, with retention of configuration. This allows synthesizing the enantiopure 2-phenylcyclopropane carboxylic acids simply starting from the commercially available enantiopure styrene oxides. Subsequent basic hydrolysis with LiOH·H_2O under MW irradiation afforded the title compounds in good overall yields (Scheme 1). When not commercially available, phosphonates were obtained by reacting triethyl phosphonoacetate with the proper alkyl bromide, in the presence of NaH as the base, from 0 °C to room temperature.[42,43] Compound **18** was commercially available.

RESULTS AND DISCUSSION

In a previous communication we have reported several small molecules capable of inhibiting *Hi*OASS-A.[38] These structures were rationally designed based on the *Hi*SAT native C-terminal pentapeptide MNLNI, which is the natural inhibitor of OASS (Figure 3). The general structure of these inhibitors relied on the presence of a carboxylic acid moiety linked through a cyclopropane linker to a side chain mimicking that of isoleucine, in a *trans* configuration. Analogues of these *β*-substituted cyclopropane carboxylic acids were prepared, and the most active compound *trans*-2-(prop-1-enyl)-cyclopropanecarboxylic acid (**17**, Figure 4) showed an encouraging K_d of 1.45 *μ*M toward *Hi*OASS-A.

However, this derivative suffered from several issues that make it particularly unsuitable for further investigation: harsh to synthesize, highly volatile, prone to decomposition in the stock

Scheme 1. Preparation of Compounds 12a−c, 13a−c, 14a−c, 15a−c, and 16a[a,b]

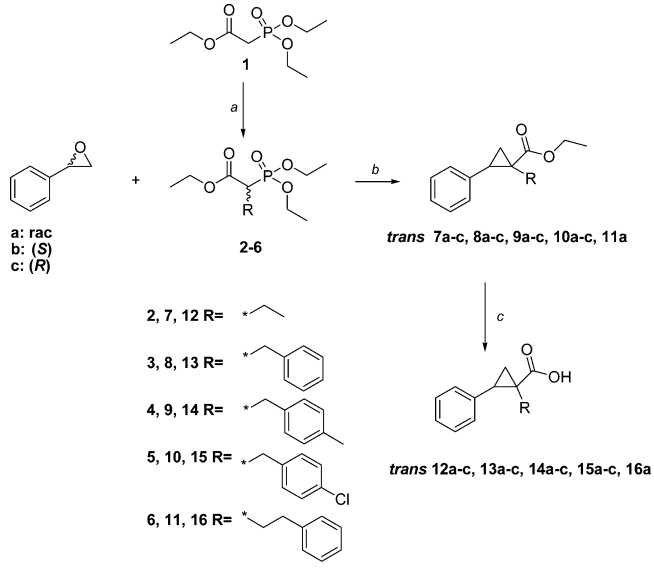

[a]Reagents and conditions: (a) R-Br, NaH, DME, 60 °C, 4 h, 54−75%; (b) n-BuLi, DME, 90 °C, 18 h, 67−76%; (c) LiOH·H_2O, THF/MeOH/H_2O (3:1:1); 10 min, MW, 86−98%. [b]For details see Table 1.

solution after a few days, hampering sometimes the reproducibility of experiments. In addition, since both the isoforms of OASS must be inhibited to obtain cysteine auxotrophs,[4] the lack of activity toward *Hi*OASS-B (unpublished observation) was considered furtherly detrimental for the development of these compounds. Taking these considerations into account, we thought that a feasible starting point for further modification of **17** was to embody the vinyl moiety into a phenyl ring, maintaining the *trans* stereorelationship with the carboxylic moiety. Besides providing an improved synthetic feasibility and stability, the insertion of a phenyl ring significantly expands the scope for further decoration and functionalization aimed at better modulating both activity and drug-likeness. When tested against OASS-A and OASS-B from *S. typhimurium*, a well characterized facultative intracellular pathogen for which both the enzyme isoforms have been thoroughly characterized,[3,5,10,12,17,44−60] this modification proved to be effective, as compound *trans*-2-phenylcyclopro-

DOI: 10.1021/acs.jmedchem.5b01775
J. Med. Chem. XXXX, XXX, XXX−XXX

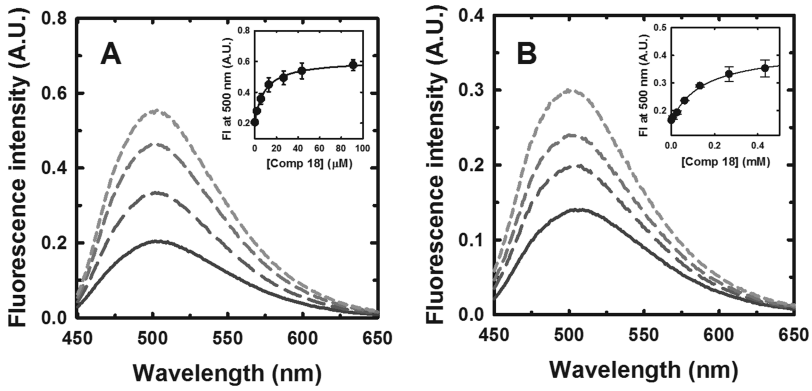

Figure 5. Binding of **18** to *St*OASS-A (A) and *St*OASS-B (**B**) as probed by the increase in the fluorescence emission of the cofactor PLP.

Table 1. Dissociation Constants of the Title Compounds for *St*OASS-A and *St*OASS-B

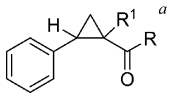

cmpd	stereochemistry	R	R^1	K_d (μM) OASS A	K_d (μM) OASS B	SI[b]
MNLNI		na[c]	na	120 ± 12	~3000	
18	*trans*	OH	H	9.2 ± 0.9	148 ± 16	16
8a	*trans*	OEt	Bn	no bind[e]	nd[f]	na
12a	*trans*	OH	Et	15 ± 1	720 ± 100	48
12b	*1R,2S*	OH	Et	12.1 ± 0.5	860 ± 90	71
12c	*1S,2R*	OH	Et	1200 ± 300	>2000	na
13a[d]	*trans*	OH	Bn	0.20 ± 0.02	4.1 ± 0.2	21
13b[g]	*1S,2S*	OH	Bn	0.067 ± 0.007	1.66 ± 0.07	25
13c	*1R,2R*	OH	Bn	50 ± 8	197 ± 27	4
14a	*trans*	OH	4-CH_3−Bn	0.077 ± 0.011	1.2 ± 0.2	16
14b	*1S,2S*	OH	4-CH_3−Bn	0.028 ± 0.005	0.49 ± 0.05	18
14c	*1R,2R*	OH	4-CH_3−Bn	81 ± 17	121 ± 12	1.5
15a	*trans*	OH	4-Cl-Bn	0.156 ± 0.007	0.76 ± 0.10	5
15b	*1S,2S*	OH	4-Cl-Bn	0.054 ± 0.008	0.42 ± 0.06	8
15c	*1R,2R*	OH	4-Cl-Bn	84 ± 10	152 ± 19	1.8
16a	*trans*	OH	PhEt	14 ± 3	27 ± 2	1.9

[a]All the compounds are in *trans* configuration. [b]SI: Selectivity index is intended as the ratio $K_{d,OASS\text{-}A}/K_{d,OASS\text{-}B}$. [c]Not attainable. [d]Stoichiometry calculated for this compound: 2.36. [e]No binding at concentrations <20 μM. The compound is not soluble in the assay buffer with 1% DMSO at concentrations >20 μM. [f]Not determined. [g]Stoichiometry calculated for this compound: 1.05.

panecarboxylic acid (**18**, Figure 4) showed moderate affinity toward *St*OASS-A, with a K_d of 9.2 μM (Figure 5A, Table 1) although toward *St*OASS-B the binding was still not statisfactory (K_d = 148 μM, Figure 5B, Table 1). Thus, with the aim of understanding which structural modification can lead to an increased affinity toward OASS-B while retaining good potency at OASS-A, **18**, along with its parent compound **17**, was docked into the active site of the two enzyme isoforms.

As expected, we observed that the hydrogen bond network established by the isoleucine of the carboxy-terminal portion of SAT (NLNI) in the crystallographic complex with *H. influenzae* OASS-A (PDB code 1Y7L) is maintained by the carboxylic group of **17** and **18** in the docking poses obtained by using the crystal structure 1OAS from *S. typhymurium* (Figure 6A). In addition, the alkyl portion of **17** and the aromatic ring of **18** are located in the small lipophilic pocket occupied by the hydrophobic portion of isoleucine. As can be appreciated in Figure 6B, a considerable portion of the binding pocket is empty. This region is characterized by the presence of a small lipophilic area surrounded by mildly polar residues.[20,33,61] Therefore, we reasoned that the functionalization of the α-carbon of the cyclopropane ring might exploit this portion of the binding site, thus establishing new interactions and increasing the binding affinity. Moreover, also in the OASS-B isoform there is space to add substituents in this direction, even if the cavity is slightly more polar (Figure 6C). Substituents at the β position of the cyclopropane ring or on the phenyl ring were not investigated, since it seems that in this region of the pocket there is no space to add other substituents, in particular considering the shape of the binding pocket of the B isoform.

Based on these observations, we designed compound **12a**, bearing an ethyl moiety at the α-carbon, which was initially prepared as racemic mixture. The affinity to *St*OASS-A did not change significantly with respect to that of **18**, whereas the affinity toward the B isoform was considerably lower ($K_{d,OASS\text{-}A}$ = 15 μM; $K_{d,OASS\text{-}B}$ = 720 μM). Since for optically active compounds the stereochemistry is usually crucial for the interaction with the enzymes, we deemed of interest to synthesize as reported in Scheme 1 the two enantiomers of **12a**. Interestingly, we found that while the *1R,2S* enantiomer **12b**

DOI: 10.1021/acs.jmedchem.5b01775
J. Med. Chem. XXXX, XXX, XXX−XXX

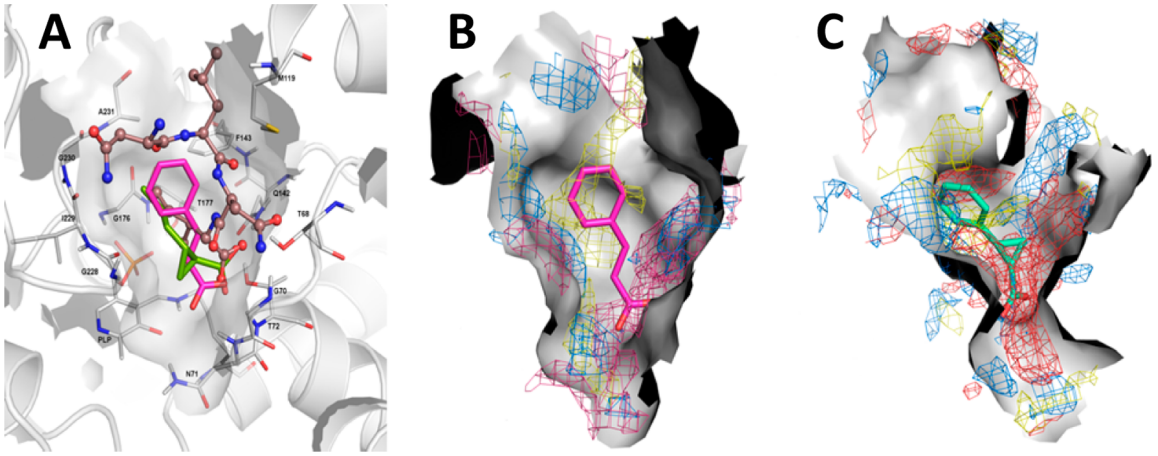

Figure 6. Binding of **18** to *St*OASS-A. (A) binding mode of **18** in *St*OASS-A binding site (1OAS crystal structure, in magenta), superposed to the previously identified compound **17** (in green) and to the C-terminal portion of CysE as solved in 1Y7L crystal structure from *H. influenzae*. (B) Map of the features of *St*OASS-A binding site with compound **18** as a reference; hydrogen bond donor areas are reported in blue meshes, the hydrogen bond acceptor in red and the hydrophobic ones in yellow. A second small hydrophobic area can be seen at the bottom of the picture, surrounded by polar areas. (C) Map of the features of *St*OASS-B binding site with compound **18** as a reference; colors are the same as in panel B).

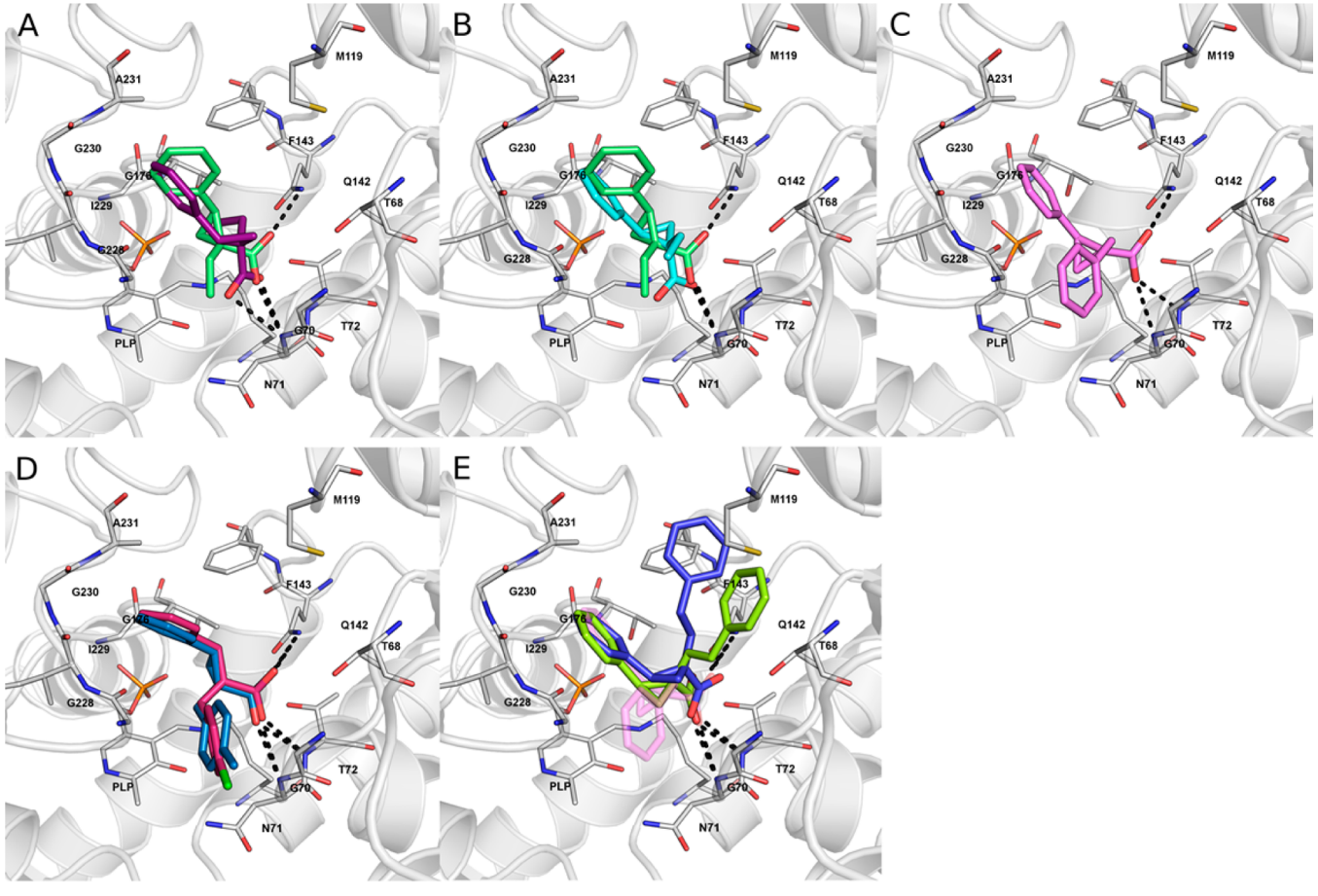

Figure 7. Stereochemical preferences for the binding of cyclopropane carboxylic acid derivatives to *St*OASS-A. (A) Two possible binding modes for compound **12b** (*1R,2S*); the one represented in green seems to be the preferred one (see text). (B) Docking pose of the inactive compound **12c** (*1S,2R*, in cyan) compared to the active enantiomer **12b**: the carboxylic group establishes fewer hydrogen bonds and the position of the aromatic ring causes some steric clashes with the residues in proximity to the compound. (C) Docking pose for compound **13b** (*1S,2S*); the additional aromatic moiety is located in the small lipophilic region. (D) Docking poses of derivatives **14b** (*1S,2S*, blue) and **15b** (*1S,2S* pink). (E) Docking poses of one of the enantiomers of **16a** (in slate blue and lime green), superposed to **13b** (in pink, transparent): the ethyl spacer is too long to allow a perfect matching of the aromatic ring with the small hydrophobic area; therefore, the derivative seems to adopt a different conformation inside the binding site, in agreement with the loss of affinity observed for this compound.

DOI: 10.1021/acs.jmedchem.5b01775
J. Med. Chem. XXXX, XXX, XXX−XXX

was barely as active as the racemic mixture, the *1S,2R* enantiomer **12c** was inactive.

The orientation of **12c** in the binding site, as obtained by docking of the compound into *St*OASS-A active site, is slightly turned compared to the active enantiomer **12b** (Figure 7A and B). This leads to a less efficient interaction of the carboxylic acid with the surrounding residues and to some steric clashes in the hydrophobic pocket occupied by the phenyl ring. Therefore, we can assume that this enantiomer is not properly accommodated inside the binding site, partially explaining the huge difference measured in the K_ds for the two compounds. With regard to **12b**, given the small size of the ligand and the big cavity of the binding site, docking studies found two equally possible binding modes (Figure 7a). In both cases, the carboxylic group is involved in a hydrogen bond network and van der Waals interactions with the phenyl ring and the ethyl group. Although it can be speculated that the first interaction is the most likely, as it resembles that of the parent pentapeptide, we took advantage of the fairly high binding constant of **12b** to carry out saturation transfer difference (STD) measurements (see details in Supporting Information). STD is a NMR spectroscopic method allowing transfer of transient energy from a protein to its ligand. The distribution of saturation transferred to the ligand protons reveals the relative spatial proximity of moieties of the ligand to the protein. This information is used to determine which part of the ligand molecule is responsible for binding, assuming that the higher the STD effect, the closer the ligand proton is to the receptor surface, and, therefore, the stronger the ligand−protein interaction.[62,63] To simplify the STD data analysis, the saturation received by the different ligand protons is expressed as group epitope mapping (GEM), i.e., percentage of STD signals normalized with respect to the most saturated signal. The higher the value, the more intimate the recognition of the ligand portion is by the protein binding pocket.[64] From experimental GEM values for compound **12b** (Figure 8A), it can be seen that the β-carbon of the cyclopropane ring represents the portion of the ligand that is more deeply buried inside the cavity and the ring hydrogens exhibit the highest saturation. Ethyl and phenyl groups seem to be only partially shielded from the solvent inside the binding pocket. CORCEMA-ST (complete relaxation and conformational exchange matrix analysis of saturation transfer)[65] theory was used to assess the agreement between the docking poses selected for compound **12b** and the corresponding STD spectrum. CORCEMA-ST calculates the predicted STD-NMR intensities for a proposed molecular model of a ligand−protein complex. The predicted STD intensities are expressed as GEM values and compared with the experimental data (Figure 8B).

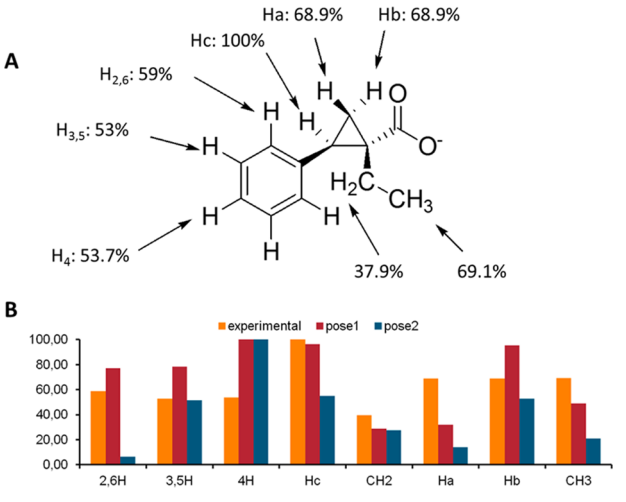

Figure 8. (A) GEM values for compound **12b** (*1R,2S*) from the experimental STD experiments. (B) The histogram compares the experimental STD values of **12b** (*1R,2S*) (in orange) to those predicted for the docking poses (in red and blue).

The first proposed binding mode (Figure 7A, in green) shows that predicted GEM values are more consistent (75% of the analyzed protons, Pose 1, Figure 8A) with the experimentally measured GEM values with respect to the second binding mode (Pose 2, Figure 8A). First of all, the GEM value obtained for the hydrogen atom bound to the β-carbon of the cyclopropane ring (H_c) reveals that the docking pose is fully in agreement with the experimental value, predicting this region as being very close to the binding site surface with stable van der Waals interactions. Moreover, similar intermediate GEM values are predicted for the ethyl moiety. Small differences are found for the aromatic portion and the hydrogen atoms in γ position of the cyclopropane ring. In particular, concerning the aromatic ring, docking results predict a more buried pose compared to the experimental findings, in particular for the *para* position. It can be hypothesized that these differences are due to the proximity of the two portions of the ligand to the flexible loop delimiting the binding pocket. This loop can adopt different conformations in solution, and the observed STD signals are realistically an average of the different conformations, whereas in the docking experiments the conformation of this loop is fixed. To take into account accurately the behavior of this loop and the influence of protein dynamics on the predicted STD values is beyond the aim of this work and will be tackled separately. The predicted GEM values for the second possible binding mode (Figure 7A, purple) are substantially different from the experimental ones, with a GEM value of only 55% for the hydrogen atom of the β-carbon of the cyclopropane ring, suggesting that this binding mode is probably not the one adopted in the formation of the protein−ligand complex.

With the aim of gaining further insight into the correct position of the 2-phenylcyclopropane carboxylic acid backbone and to further exploit the available volume inside the binding site to increase the binding affinity, we synthesized a compound bearing a benzyl group at the α-carbon. This substituent might stabilize the binding mode in the most favorable pose, occupying the portion of the binding site that is left empty by smaller ligands. We reasoned that an aromatic group at the α-carbon could be well allocated in this region characterized by a small hydrophobic area surrounded by polar residues, defining mildly polar areas. Moreover, the aromatic group leaves space for easily adding further substituents and maximizing the complementarity with the binding site. Therefore, compounds **13a** and its enantiomeric pure analogues **13b** (*1S,2S*) and **13c** (*1R,2R*) were synthesized and tested. The racemic mixture exhibited a very good activity compared to the ethyl derivative and, of the two enantiomers, **13b** was found to show high affinity to both *St*OASS-A and *St*OASS-B with K_ds in the nanomolar and low micromolar ranges, respectively (Table 1). On the other hand, **13c**, as expected, was found to be several-fold (700-fold) less potent than the corresponding enantiomer for *St*OASS-A. The enantiomeric preferences were further confirmed by calculation of the binding stoichiometry to

DOI: 10.1021/acs.jmedchem.5b01775
J. Med. Chem. XXXX, XXX, XXX−XXX

*St*OASS-A. In the case of the racemic mixture the binding stoichiometry is about 2 and decreases to about 1 when compound **13b** is used for the titration. In fact, one molecule of **13b** binds for each active site of StOASS-A, whereas 2 molecules of the racemic mixture **13a** are needed, since it is a 50:50 mixture of **13b** and **13c**. The docking of **13b** into the binding pocket of *St*OASS-A gave us other useful information (Figure 7C). First, it allowed identifying the binding mode of the 2-phenylcyclopropane carboxylic acid backbone within the binding site. This is helpful in order to carry out further ligand optimization via decoration of the 2-phenyl ring with various functional groups. Second, the analysis of the pose of **13b** led us to speculate that there is further room for additional small functional groups in the *para* position of the α-benzyl ring. Therefore, compounds bearing at the *para* position of the benzyl ring either an electron donor group, such as the methyl, or an electron withdrawing group, such as chlorine, were synthesized and tested. First, we synthesized the *1S,2S* enantiomers **14b** and **15b**, assuming that also in this case this stereochemistry would have been the preferred one. However, we deemed it of interest to also prepare the racemic derivatives **14a** and **15a** and the enantiomers *1S,2S* **14c** and **15c**, in order to further corroborate, with additional data, the most favorable stereochemistry (Table 1, Figure 7D). Moreover, since the pocket accommodating the benzyl ring seemed to be large, we also synthesized the α-phenylethyl derivative **16a**, in which the aromatic ring is connected to the α-carbon of the cyclopropane through an ethyl spacer. We found that, compared to **13b**, the affinities of **14b** and **15b** toward *St*OASS-A were almost the same. However, both compounds showed a more than 3-fold improved affinity toward *St*OASS-B, with K_ds in the low nanomolar range. To our knowledge, this represents the strongest binder reported so far for the B isoform of *St*OASS. In fact, a previously identified small molecule compound active on *St*OASS-B[21] exhibited dissociation constants for the B isoform of about 30 μM, about 70-fold higher than the best compound here identified. As expected, for what concerned *St*OASS-A, the activity can be ranked based on the absolute configuration as follows: *1S,2S* > *rac* ≫ *1R,2R*. Compound **16a** was only marginally active. It can be speculated that the phenylethyl substituent affects the interaction of the whole molecule since the ethyl linker is too long to allow the accommodation of the phenyl ring in the small lipophilic area occupied by the benzyl group. Therefore, for both the enantiomers of **16a** the phenylethyl moiety points toward the other side of the binding site, where the C-terminal residues of CysE in the 3IQG crystal structure from *Hi*OASS-A bind (Figure 7E). The importance of the acid group and its interactions in the pocket of the binding site is further corroborated by the lack of activity of the ester derivative **8a**.

Preliminary Structure Activity Relationships (SAR). Although the set of compounds synthesized is relatively small, some preliminary hints of SAR can be described. The vinyl moiety of **17** can be embodied in a phenyl ring and kept in a *trans* conformation with respect to the carboxylic acid moiety. Trapping the acid group into an ester leads to a severe decrease or even loss of the activity. Substitution at the α-carbon of the cyclopropane not only is well tolerated, as in the case of the compound **12a**, but it also remarkably enhances the affinity toward both *St*OASS-A and *St*OASS-B, as in the case of the α-benzyl substitution. Elongating the spacer between the phenyl ring and the α-carbon of cyclopropane from one to two methylene units leads to a loss of activity (**16**, $K_{d,OASS\text{-}A}$ = 14 μM). The same effect is recorded with the deletion of the aromatic ring (**12a**, $K_{d,OASS\text{-}A}$ = 15 μM; **12b**, $K_{d,OASS\text{-}A}$ = 12.1 μM). The benzyl ring, along with positioning the 2-phenylcyclopropane carboxylic acid into its most favorable pose for interaction, is probably responsible for the $\pi-\pi$ interaction. Moreover, the benzyl ring can be further decorated with small functional groups, such as methyl and chlorine, regardless of their electron-donor or electron-withdrawing properties. In this first round of modifications, only the *para* position was investigated. However, a medicinal chemistry campaign aimed at refining the SAR for these derivatives is currently underway in our laboratory. Stereochemistry was found to be pivotal for ensuring high affinity. In the case of the α-ethyl substituted derivatives, the levorotatory enantiomer *1R,2S* was found to be more than 1000-fold less active than the counterpart. In the case of the α-benzyl substitution, the dextrorotatory enantiomer *1S,2S* shows consistently an affinity higher than that of other isomers, according to the following trend: *1S,2S* > *rac* ≫ *1R,2R*. Therefore, the most active compounds are those showing a *2S* stereochemistry in their structure. This is an important finding to consider in the planning of further derivatives. Indeed, since the synthetic method of cyclopropanation maintains the configuration of the starting epoxides, it can be speculated that (*S*)-styrene oxides will yield the active derivatives.

Selectivity of the Compounds toward the Two *St*OASS Isoforms. As described above, inhibition of both isoforms of *St*OASS is important for granting a complete inhibition of cysteine biosynthesis in bacteria. In this work, we have obtained an excellent activity toward *St*OASS-B, especially with compounds **15b** and **14b**. However, considering that the ultimate target of our work is a compound showing the same activity toward both isoforms, we have rationalized the information collected in this work on the basis of the ratio between *St*OASS-B and *St*OASS-A affinities (Table 1). First, it must be noticed that, in general, the affinity toward *St*OASS-B is proportional to that for *St*OASS-A, although always weaker (Figure S2). Therefore, we focused on the increase in the activity toward the A isoform. When the α-carbon is not substituted, the ratio between the activity to *St*OASS-B and *St*OASS-A is around 16 (see compound **18**). Substitution with an ethyl group, although maintaining the activity toward the A isoform, led to a sharp decrease in the affinity toward the B isoform (see **12a** and **12b**, with an affinity ratio of around 50 and 70, respectively). Substitution with the α-benzyl group reduces the activity ratio compared to the α-ethyl, but such a ratio still remains around 20 in the case of the racemic mixture and 25 for the more active enantiomer. What seems to remarkably improve the affinity ratio is the insertion of a lipophilic substituent at the *para* position of the benzyl ring. Indeed, for those compounds bearing a *para*-chloro substitution, that is **15a** and **15b**, the K_d for *St*OASS-B is only 5- and 8-fold higher than that for *St*OASS-A, respectively. Although a higher number of derivatives will shed more light into the SAR of these inhibitors, we can conclude that the α-benzyl substitution leads not only to the strongest compounds toward *St*OASS-A and *St*OASS-B so far identified, but also, if properly substituted, to the loss of selectivity between the two isoforms.

Inhibitory Activity of Compounds 15b and 15c toward the Two *St*OASS Isoforms. After characterizing the compounds with regard to their SAR, we investigated whether there was a direct correlation between the binding affinities and the enzyme inhibitory activity. Indeed, it is

DOI: 10.1021/acs.jmedchem.5b01775
J. Med. Chem. XXXX, XXX, XXX−XXX

expected that for compounds that act as competitive inhibitors K_d coincides with K_i. Compound **15b** was selected for the inhibition assay because of its high binding activity and its low selectivity toward the two enzyme isoforms *St*OASS-A and B. The dependence of the fractional activity on **15b** concentration is reported in SI Figure S3 and the calculated IC_{50}s are reported in Table 2. As expected for a compound that binds to the

Table 2. IC_{50}s of Representative Inhibitors of *St*OASS-A and *St*OASS-B

	OASS-A		OASS-B	
cmpd	K_d (μM)	IC_{50} (μM)	K_d (μM)	IC_{50} (μM)
15b	0.054 ± 0.008	0.099 ± 0.004	0.42 ± 0.06	0.50 ± 0.03
15c	84 ± 10	14 ± 1	152 ± 19	48 ± 2

enzyme active site and competes with the substrate OAS, compound **15b** was found to inhibit both isoforms of *St*OASS with an IC_{50} comparable to the dissociation constants calculated by the direct fluorimetric titration (K_d *St*OASS-A = 0.054 μM ± 0.008 vs IC_{50} *St*OASS-A = 0.099 μM ± 0.004; K_d *St*OASS-B = 0.42 μM ± 0.06 vs IC_{50} *St*OASS-B = 0.50 μM ± 0.03). A similar conclusion can be drawn for the *1R,2R* isomer, which exhibits a lower affinity for the enzyme. Therefore, we have demonstrated that there is a direct correlation between ligand binding and inhibition for both the isoforms.

CONCLUSIONS

Inhibition of cysteine biosynthesis may strongly affect the life cycle of many unicellular microorganisms and plants. *O*-Acetylserine sulfhydrylase catalyzes the last step of cysteine biosynthesis, allowing the transfer of sulfide to acetylserine. Since mammals are not equipped with this enzyme, supplying cysteine through the reverse transsulfuration pathway from methionine, inhibitors of OASS would be highly selective and safe. Taking into account the data from our previous efforts,[38] and combining computational and spectroscopic approaches such as STD NMR, we have rationally designed and synthesized a series of 2-phenylcyclopropane carboxylic acids to be tested against *St*OASS-A and *St*OASS-B. Overall, this medicinal chemistry campaign led to derivatives about 4000-fold and 7000-fold more active on StOASS-A and StOASS-B, respectively, than the peptidic inhibitor MNLNI, and to a reduction of the selectivity toward the two isoforms. Moreover, we have demonstrated that compounds that bind to the enzyme active site are inhibitors of both the isoforms efficiently competing with the substrate. Given the various range of K_ds, a preliminary hint of structure−activity relationships could be outlined. The carboxylic acid moiety is crucial for the activity, as its substitution with an ester led to loss of activity. The cyclopropane ring, that maintains in the suitable *trans* configuration the carboxylic acid moiety and the phenyl ring, proved to be a valuable structural solution, confirming the results of our previous investigations. Substitution at the α-carbon of the cyclopropane strongly affects both the potency of the compounds and their selectivity toward the two isoforms *St*OASS-A and *St*OASS-B. Bulky groups such as the *para* substituted and unsubstituted benzyl moieties allow to obtain potent inhibitors. However, a substituent such as chlorine at the *para* position of the benzyl ring allows a strong affinity to be coupled with a reduction of selectivity toward the two isoforms of *St*OASS, with the K_d toward OASS-B only 8 times higher than that toward OASS-A. Interestingly, the stereochemistry is extremely important in conferring high potency, and the enantiomer *1S,2S* is more potent than the *1R,2R* counterpart by an average 1000-fold factor. Finally, to the best of our knowledge, **14b** and **15b** are the most active compounds described so far toward *St*OASS-B. Altogether, these findings provide a solid base to further investigate this series of 2-phenylcyclopropane carboxylic acids as a valuable tool to tune the events associated with the biosynthesis of cysteine in unicellular organisms, such as bacterial virulence and drug resistance.

EXPERIMENTAL SECTION

General Information. All the reagents were purchased from Sigma-Aldrich, Alfa-Aesar, and Enamine at reagent purity and, unless otherwise noted, were used without any further purification. Dry solvents used in the reactions were obtained by distillation of technical grade materials over appropriate dehydrating agents. MCRs were performed using CEM Microwave Synthesizer-Discover model. Reactions were monitored by thin layer chromatography on silica gel-coated aluminum foils (silica gel on Al foils, SUPELCO Analytical, Sigma-Aldrich) at 254 and 365 nm. Where indicated, intermediates and final products were purified by silica gel flash chromatography (silica gel, 0.040−0.063 mm), using appropriate solvent mixtures.

^{1}H NMR and ^{13}C NMR spectra were recorded on a BRUKER AVANCE spectrometer at 400 and 100 MHz, respectively, with TMS as internal standard. For STD experiments please refer to the Supporting Information. ^{1}H NMR spectra are reported in this order: multiplicity and number of protons. Standard abbreviation indicating the multiplicity were used as follows: s = singlet, d = doublet, dd = doublet of doublets, t = triplet, q = quadruplet, m = multiplet, and br = broad signal. HPLC/MS experiments were performed with an Agilent 1100 series HPLC apparatus, equipped with a Waters Symmetry C18, 3.5 μm, 4.6 mm × 75 mm column and an MS: Applied Biosystem/MDS SCIEX instrument, with API 150EX ion surce. HRMS experiments were performed with an LTQ ORBITRAP XL THERMO apparatus.

All compounds were tested as 95% purity or higher (by HPLC/MS).

General Procedure for the Synthesis of Phosphonates (2−6). Ethyl 2-(diethoxyphosphoryl)acetate (1 equiv) was added dropwise to a cooled suspension of NaH (1.1 equiv) in dry DME (2 mL/mmol). After stirring at 25 °C for 2 h the appropriate halide (1.1 equiv) was added, and the mixture was heated at 60 °C for 2 h. The reaction mixture was poured into ice water and extracted with ethyl acetate and the combined organic layers were washed with H_2O and brine, dried over Na_2SO_4, and evaporated under reduced pressure. The crude material was purified through flash chromatography eluting with dichloromethane/diethyl ether 95:5 to give the desired compounds as colorless oil in yields ranging from 54% to 68%. Analytical data for compounds **5a**, **b**, and **e** matched the data already published.[41−43]

General Procedure for the Cyclopropanation. To a solution of the appropriate phosphonate (2 equiv) in dry DME (5 mL/mmol) at 25 °C, *n*-buthyllithium (2.5 M in hexane, 2 equiv) was added dropwise over 5 min. After stirring at the same temperature for 30 min, the appropriate styrene oxide (1 equiv) was added portionwise and the mixture heated at 90 °C for 18 h. After cooling, saturated aqueous solution of NH_4Cl was added and the organic layers were extracted with ethyl acetate (3 × 10 mL), washed with brine, dried over anhydrous Na_2SO_4, and evaporated under reduced pressure. The oil obtained was purified through flash column chromatography eluting with petroleum ether/ethyl acetate (95:5), to give the desired product as yellowish oil in yields ranging from 65% to 78%.

General Procedure for the Ester Hydrolysis: Synthesis of Compounds 12a−c, 13a−c, 14a−c, 15a−c, and 16a. Esters **7a−c**, **8a−c**, **9a−c**, **10a−c**, and **11a** (1 equiv) and $LiOH·H_2O$ (4 equiv) were dissolved in a solution of THF/MeOH/H_2O (3/1/1, 1 mL/mmol) and heated under stirring in a microwave oven at 100 °C for 7 min. The reaction mixture is then evaporated *in vacuo*, and the crude is

DOI: 10.1021/acs.jmedchem.5b01775
J. Med. Chem. XXXX, XXX, XXX−XXX

taken up with H_2O, acidified with HCl 1 N, and extracted with ethyl acetate, that is in turn washed with brine and dried over anhydrous Na_2SO_4. After the evaporation of the solvent the crude material was purified through flash column chromatography eluting dichloromethane/methanol (95:5), to give the desired product as a white solid in yields ranging from 56% to 67%.

*trans-1-Ethyl-2-phenylcyclopropanecarboxylic acid (**12a**).* ^{1}H NMR (300 MHz, $CDCl_3$): 7.43−7.36 (m, 5H); 3.20 (d, J = 15.72, 1H); 3.02 (t, J = 8.34, 1H); 2.13−1.97 (m, 2H); 1.51−1.47 (m, 1H); 0.80 (t, J = 7.32 Hz, 3H). ^{13}C NMR (100.6 MHz, $CDCl_3$): 129.29; 128.21; 126.87; 33.32; 31.17; 21.48; 18.49; 11.59. HRMS (ESI) calculated for $C_{12}H_{14}O_2$ ([M-H]$^-$) 190.0994; found 190.1002.

*(1R,2S)-1-Ethyl-2-phenylcyclopropanecarboxylic acid (**12b**).* ^{1}H NMR (300 MHz, $CDCl_3$): 7.43−7.36 (m, 5H); 3.20 (d, J = 15.72, 1H); 3.02 (t, J = 8.34, 1H); 2.13−1.97 (m, 2H); 1.51−1.47 (m, 1H); 0.80 (t, J = 7.32 Hz, 3H). ^{13}C NMR (100.6 MHz, $CDCl_3$): 129.29; 128.21; 126.87; 33.32; 31.17; 21.48; 18.49; 11.59. $[\alpha]^{20}_D$ − 100.77 (c 1, $CHCl_3$), HRMS (ESI) calculated for $C_{12}H_{14}O_2$ ([M-H]$^-$) 190.0994; found 190.0998.

*(1S,2R)-1-Ethyl-2-phenylcyclopropanecarboxylic acid (**12c**).* ^{1}H NMR (300 MHz, $CDCl_3$): 7.43−7.36 (m, 5H); 3.20 (d, J = 15.72, 1H); 3.02 (t, J = 8.34, 1H); 2.13−1.97 (m, 2H); 1.51−1.47 (m, 1H); 0.80 (t, J = 7.32 Hz, 3H). ^{13}C NMR (100.6 MHz, $CDCl_3$): 129.29; 128.21; 126.87; 33.32; 31.17; 21.48; 18.49; 11.59. $[\alpha]^{20}_D$ + 100.77 (c 1, $CHCl_3$), HRMS (ESI) calculated for $C_{12}H_{14}O_2$ ([M-H]$^-$) 190.0994; found 190.1010.

*trans-1-Benzyl-2-phenylcyclopropanecarboxylic acid (**13a**).* ^{1}H NMR (300 MHz, $CDCl_3$): 7.39−7.20 (m, 10H); 3.20 (d, J = 15.72, 1H); 3.02 (t, J = 8.34, 1H); 2.00−1.93 (m, 2H); 1.51−1.47 (m, 1H). ^{13}C NMR (100.6 MHz, $CDCl_3$): 181.64; 139.98; 136.22; 129.39; 128.73; 128.49; 128.21; 127.26; 126.04; 34.09; 32.93; 30.73; 18.49. HRMS (ESI) calculated for $C_{17}H_{16}O_2$ ([M-H]$^-$) 252.3077; found 252.3202.

*(1S,2S)-1-Benzyl-2-phenylcyclopropanecarboxylic acid (**13b**).* ^{1}H NMR (300 MHz, $CDCl_3$): 7.39−7.20 (m, 10H); 3.20 (d, J = 15.72, 1H); 3.02 (t, J = 8.34, 1H); 2.00−1.93 (m, 2H); 1.51−1.47 (m, 1H). ^{13}C NMR (100.6 MHz, $CDCl_3$): 181.64; 139.98; 136.22; 129.39; 128.73; 128.49; 128.21; 127.26; 126.04; 34.09; 32.93; 30.73; 18.49. $[\alpha]^{20}_D$ − 25.88 (c 1, $CHCl_3$), HRMS (ESI) calculated for $C_{17}H_{16}O_2$ ([M-H]$^-$) 252.3077; found 252.3158.

*(1R,2R)-1-Benzyl-2-phenylcyclopropanecarboxylic acid (**13c**).* ^{1}H NMR (300 MHz, $CDCl_3$): 7.39−7.20 (m, 10H); 3.20 (d, J = 15.72, 1H); 3.02 (t, J = 8.34, 1H); 2.00−1.93 (m, 2H); 1.51−1.47 (m, 1H). ^{13}C NMR (100.6 MHz, $CDCl_3$): 181.64; 139.98; 136.22; 129.39; 128.73; 128.49; 128.21; 127.26; 126.04; 34.09; 32.93; 30.73; 18.49. $[\alpha]^{20}_D$ + 25.88 (c 1, $CHCl_3$), HRMS (ESI) calculated for $C_{17}H_{16}O_2$ ([M-H]$^-$) 252.3077; found 252.3200.

*trans-1-(4-Methylbenzyl)-2-phenylcyclopropanecarboxylic acid (**14a**).* ^{1}H NMR (300 MHz, $CDCl_3$): 7.39−7.20 (m, 5H); 7.11 (d, J = 8.43, 4H); 3.20 (d, J = 15.72, 1H); 3.02 (t, J = 8.34, 1H); 2.25 (s, 3H); 2.00−1.93 (m, 2H); 1.51−1.47 (m, 1H). ^{13}C NMR (100.6 MHz, $CDCl_3$): 181.64; 139.98; 136.22; 129.39; 128.73; 128.49; 128.21; 127.26; 126.04; 34.09; 32.93; 30.73; 18.49; 11.59. HRMS (ESI) calculated for $C_{18}H_{18}O_2$ ([M-H]$^-$) 266.3343; found 266.3206.

*(1S,2S)-1-(4-Methylbenzyl)-2-phenylcyclopropanecarboxylic acid (**14b**).* ^{1}H NMR (300 MHz, $CDCl_3$): 7.39−7.20 (m, 5H); 7.11 (d, J = 8.43, 4H); 3.20 (d, J = 15.72, 1H); 3.02 (t, J = 8.34, 1H); 2.25 (s, 3H); 2.00−1.93 (m, 2H); 1.51−1.47 (m, 1H). ^{13}C NMR (100.6 MHz, $CDCl_3$): 181.64; 139.98; 136.22; 129.39; 128.73; 128.49; 128.21; 127.26; 126.04; 34.09; 32.93; 30.73; 18.49; 11.59. $[\alpha]^{20}_D$ − 110.9 (c 1, $CHCl_3$), HRMS (ESI) calculated for $C_{18}H_{18}O_2$ ([M-H]$^-$) 266.3343; found 266.4008.

*(1R,2R)-1-(4-Methylbenzyl)-2-phenylcyclopropanecarboxylic acid (**14c**).* ^{1}H NMR (300 MHz, $CDCl_3$): 7.39−7.20 (m, 5H); 7.11 (d, J = 8.43, 4H); 3.20 (d, J = 15.72, 1H); 3.02 (t, J = 8.34, 1H); 2.25 (s, 3H); 2.00−1.93 (m, 2H); 1.51−1.47 (m, 1H). ^{13}C NMR (100.6 MHz, $CDCl_3$): 181.64; 139.98; 136.22; 129.39; 128.73; 128.49; 128.21; 127.26; 126.04; 34.09; 32.93; 30.73; 18.49; 11.59. $[\alpha]^{20}_D$ + 110.9 (c 1, $CHCl_3$), HRMS (ESI) calculated for $C_{18}H_{18}O_2$ ([M-H]$^-$) 266.3343; found 266.3288.

*trans-1-(4-Chlorobenzyl)-2-phenylcyclopropanecarboxylic acid (**15a**).* ^{1}H NMR (300 MHz, $CDCl_3$): 7.39−7.11 (m, 9H); 3.20 (d, J = 15.72, 1H); 3.02 (t, J = 8.34, 1H); 2.00−1.93 (m, 2H); 1.51−1.47 (m, 1H). ^{13}C NMR (100.6 MHz, $CDCl_3$): 181.64; 139.98; 136.22; 129.39; 128.73; 128.49; 128.21; 127.26; 126.04; 34.09; 32.93; 30.73; 18.49; HRMS (ESI) calculated for $C_{17}H_{15}ClO_2$ ([M-H]$^-$) 286.7528; found 286.8022.

*(1S,2S)-1-(4-Chlorobenzyl)-2-phenylcyclopropanecarboxylic acid (**15b**).* ^{1}H NMR (300 MHz, $CDCl_3$): 7.39−7.11 (m, 9H); 3.20 (d, J = 15.72, 1H); 3.02 (t, J = 8.34, 1H); 2.00−1.93 (m, 2H); 1.51−1.47 (m, 1H). ^{13}C NMR (100.6 MHz, $CDCl_3$): 181.64; 139.98; 136.22; 129.39; 128.73; 128.49; 128.21; 127.26; 126.04; 34.09; 32.93; 30.73; 18.49. $[\alpha]^{20}_D$ − 40.77 (c 1, $CHCl_3$), HRMS (ESI) calculated for $C_{17}H_{15}ClO_2$ ([M-H]$^-$) 286.7528; found 286.7686.

*(1R,2R)-1-(4-Chlorobenzyl)-2-phenylcyclopropanecarboxylic acid (**15c**).* ^{1}H NMR (300 MHz, $CDCl_3$): 7.39−7.11 (m, 9H); 3.20 (d, J = 15.72, 1H); 3.02 (t, J = 8.34, 1H); 2.00−1.93 (m, 2H); 1.51−1.47 (m, 1H). ^{13}C NMR (100.6 MHz, $CDCl_3$): 181.64; 139.98; 136.22; 129.39; 128.73; 128.49; 128.21; 127.26; 126.04; 34.09; 32.93; 30.73; 18.49. $[\alpha]^{20}_D$ + 40.77 (c 1, $CHCl_3$), HRMS (ESI) calculated for $C_{17}H_{15}ClO_2$ ([M-H]$^-$) 286.7528; found 286.7682.

*trans-1-Phenethyl-2-phenylcyclopropanecarboxylic acid (**16a**).* ^{1}H NMR (300 MHz, $CDCl_3$): 7.39−7.20 (m, 10H); 3.02 (t, J = 8.34, 1H); 3.01−2.89 (m, 1H); 2.78−2.68 (m, 1H); 2.63−2.53 (m, 1H); 2.37−2.21 (m, 1H); 2.20−2.10 (m, 1H); 1.51−1.47 (m, 1H). ^{13}C NMR (100.6 MHz, $CDCl_3$): 181.64; 139.98; 136.22; 129.39; 128.73; 128.49; 128.21; 127.26; 126.04; 34.09; 32.93; 30.73; 18.49; 15.23. HRMS (ESI) calculated for $C_{18}H_{18}O_2$ ([M-H]$^-$) 266.1307; found 266.2286.

Molecular Modeling. For docking studies, chain A of the crystal structures of OASS-A (pdb 1OAS) and OASS-B (pdb 2JC3) from *Salmonella typhimurium* were used. Protein structures were prepared using the wizard tool available from the Schrodinger suite. Ligands were prepared using the LigPrep tool of the Schrodinger suite at pH 7.5 ± 1. Docking studies were performed using PLANTS induced fit approach, allowing some selected residues of the binding pocket to move during ligand binding. The following residues were selected: for OASS-A: E66, T68, N69, N71, T72, R99, M119, Q142, P143, V175, T177, I229; for OASS-B: E66, T68, S69, N71,T72, R99, M119, Q140, F141, M173, T175, I209, R210, R211, W212.

NMR Measurements for STD Experiments. NMR spectra were acquired on a Varian (Agilent Technologies) Inova 600 NMR Spectrometer at 20 °C, on samples with a molar excess of 1:300 (OASS-A: *1R,2S*-(−)-**12b**). Ligand concentration was kept at 3 mM in the presence of 10 μM protein and were dissolved in phosphate buffer pH 8.0 (5 mM K_2PO_4, 3% DMSO-d_6).

Saturation transfer difference (STD) experiments were collected with 64 K data points in the direct dimension and 512 scans in a spectral window of 7000 Hz. The water signal was suppressed by the excitation sculpting method (dpfgse_water). Selective saturation of the protein resonances (on resonance spectrum) was performed by irradiating at −0.9 ppm using Gaussian-shaped pulses for a saturation time of 3 s. For the reference spectrum (off resonance), the samples were irradiated at 26.6 ppm. NMR data were processed and analyzed using MestReNova 8.1 software. Group epitope mapping (GEM) was calculated setting the highest STD intensity to 100% and all other STD signals were calculated accordingly.

All CORCEMA calculations were carried out using CORCEMA SX 3.8.[65−67] Protein residues within 7 Å distance of the ligand were included for the calculation of theoretical STD effects. Ligand and protein concentrations, their equilibrium constant, and spectrometer frequency were all set according to experimental values. The free ligand rotational correlation time was estimated to be 0.3 ns. The bound ligand rotational correlation time was 32 ns. Because protein signals around 0 ppm were selectively irradiated for the STD experiment, all methyl protons in the enzyme were assumed to be saturated. STD intensities of nonexchangeable protons on ligand were calculated at a saturation time of 3 s.

DOI: 10.1021/acs.jmedchem.5b01775
J. Med. Chem. XXXX, XXX, XXX−XXX

Ligand Binding Affinity to OASS. The binding affinity of ligands was determined by monitoring the increase in fluorescence emission of the bound coenzyme following excitation at 412 nm.[21,36] Emission spectra were recorded as a function of ligand concentration in a solution containing 0.5−1.0 μM OASS, 100 mM Hepes buffer, pH 7.0, at 20 °C. Fluorescence measurements were carried out using a FluoroMax-3 fluorometer (HORIBA), equipped with a thermostated cell-holder. The dependence of fluorescence intensity at the emission peak, 500 nm, on ligand concentration was fitted to a binding isotherm

$$I = \frac{I_{max}[L]}{K_{diss} + [L]}$$

where I is the fluorescence intensity at 500 nm in the presence of the ligand, after subtraction of the fluorescence intensity at 500 nm in the absence of the ligand, I_{max} is the maximum fluorescence change at saturating [L], [L] is the ligand concentration, and K_{diss} is the dissociation constant of the OASS-ligand complex. This measurement is a direct determination of ligand dissociation constant in the absence of substrate. For competitive inhibitors K_d coincides with K_i.

■ ASSOCIATED CONTENT

Supporting Information

The Supporting Information is available free of charge on the ACS Publications website at DOI: 10.1021/acs.jmedchem.5b01775.

^{1}H NMR description of compounds **4**, **5**, **7a-c**, **8a-c**, **9a-c**, **10a-c**, **11a**; the biological methods used for the determination of the K_ds; the method used for STD−NMR measurements (PDF)

SMILES data for compounds (CSV)

■ AUTHOR INFORMATION

Corresponding Authors

*E-mail: barbara.campanini@unipr.it. Phone: +39 0521906613.
*E-mail: gabriele.costantino@unipr.it. Phone: +39 0521905054.

Present Addresses

¶Laboratory of Medicinal Chemistry, Rega Institute for Medical Research, KU Leuven, Leuven, Belgium
△Dipartimento Oncologico e Tecnologie Avanzate - IRCCS-ASMN, Reggio Emilia, Italy

Author Contributions

■Marco Pieroni and Giannamaria Annunziato contributed equally to this work.

Author Contributions

The manuscript was written through contributions of all authors. All authors have given approval to the final version of the manuscript.

Notes

The authors declare no competing financial interest.

■ ACKNOWLEDGMENTS

The work described in this paper was partly carried out under the MSCA-ITN-2014-ETN project INTEGRATE (grant number 642620).

■ ABBREVIATIONS

CoA, Coenzyme A; GEM, group epitope mapping; MW, microwave; OASS, *O*-acetylserine sulfhydrylase; PDB, protein data bank; PLP, pyridoxal 5′-phosphate; SAR, structure−activity relationship; SAT, serine *O*-acetyltransferase; STD, saturation transfer difference

■ REFERENCES

(1) Sekowska, A.; Kung, H. F.; Danchin, A. Sulfur metabolism in *Escherichia coli* and related bacteria: facts and fiction. *J. Mol. Microbiol. Biotechnol.* **2000**, *2*, 145−177.

(2) Kredich, N. M. Regulation of L-Cysteine Biosynthesis in Salmonella Typhimurium I. effects of growth on varying sulfur sources and o-acetyl-l-serine on gene expression. *J. Biol. Chem.* **1971**, *246* (11), 3474−3484.

(3) Mozzarelli, A.; Bettati, S.; Campanini, B.; Salsi, E.; Raboni, S.; Singh, R.; Spyrakis, F.; Kumar, V. P.; Cook, P. F. The Multifaceted Pyridoxal 5′-Phosphate-Dependent O-Acetylserine Sulfhydrylase. *Biochim. Biophys. Acta, Proteins Proteomics* **2011**, *1814* (11), 1497−1510.

(4) Hulanicka, M. D.; Hallquist, S. G.; Kredich, N. M.; Mojica-A, T. Regulation of O-Acetylserine Sulfhydrylase B by L-Cysteine in Salmonella Typhimurium. *J. Bacteriol.* **1979**, *140* (1), 141−146.

(5) Tai, C. H.; Nalabolu, S. R.; Jacobson, T. M.; Minter, D. E.; Cook, P. F. Kinetic Mechanisms of the A and B Isozymes of O-Acetylserine Sulfhydrylase from Salmonella Typhimurium LT-2 Using the Natural and Alternate Reactants. *Biochemistry* **1993**, *32* (25), 6433−6442.

(6) Huang, B.; Vetting, M. W.; Roderick, S. L. The Active Site of O-Acetylserine Sulfhydrylase Is the Anchor Point for Bienzyme Complex Formation with Serine Acetyltransferase. *J. Bacteriol.* **2005**, *187* (9), 3201−3205.

(7) Oda, Y.; Mino, K.; Ishikawa, K.; Ataka, M. Three-Dimensional Structure of a New Enzyme, O-Phosphoserine Sulfhydrylase, Involved in L-Cysteine Biosynthesis by a Hyperthermophilic Archaeon, Aeropyrum Pernix K1, at 2.0Å Resolution. *J. Mol. Biol.* **2005**, *351* (2), 334−344.

(8) Fyfe, P. K.; Westrop, G. D.; Ramos, T.; Müller, S.; Coombs, G. H.; Hunter, W. N. Structure of *Leishmania Major* Cysteine Synthase. *Acta Crystallogr., Sect. F: Struct. Biol. Cryst. Commun.* **2012**, *68* (7), 738−743.

(9) Burkhard, P.; Tai, C.-H.; Ristroph, C. M.; Cook, P. F.; Jansonius, J. N. Ligand Binding Induces a Large Conformational Change in O-Acetylserine Sulfhydrylase from Salmonella typhimurium1. *J. Mol. Biol.* **1999**, *291* (4), 941−953.

(10) Burkhard, P.; Jagannatha Rao, G. S.; Hohenester, E.; Schnackerz, K. D.; Cook, P. F.; Jansonius, J. N. Three-Dimensional Structure of O-Acetylserine Sulfhydrylase from Salmonella typhimurium1. *J. Mol. Biol.* **1998**, *283* (1), 121−133.

(11) Bonner, E. R.; Cahoon, R. E.; Knapke, S. M.; Jez, J. M. Molecular Basis of Cysteine Biosynthesis in Plants: structural and functional analysis of o-acetylserine sulfhydrylase from arabidopsis thaliana. *J. Biol. Chem.* **2005**, *280* (46), 38803−38813.

(12) Tai, C.-H.; Burkhard, P.; Gani, D.; Jenn, T.; Johnson, C.; Cook, P. F. Characterization of the Allosteric Anion-Binding Site of O-Acetylserine Sulfhydrylase†. *Biochemistry* **2001**, *40* (25), 7446−7452.

(13) Schnell, R.; Oehlmann, W.; Singh, M.; Schneider, G. Structural Insights into Catalysis and Inhibition of O-Acetylserine Sulfhydrylase from Mycobacterium Tuberculosis: crystal structures of the enzyme α-aminoacrylate intermediate and an enzyme-inhibitor complex. *J. Biol. Chem.* **2007**, *282* (32), 23473−23481.

(14) Raj, I.; Kumar, S.; Gourinath, S. The Narrow Active-Site Cleft of *O* -Acetylserine Sulfhydrylase from *Leishmania Donovani* Allows Complex Formation with Serine Acetyltransferases with a Range of C-Terminal Sequences. *Acta Crystallogr., Sect. D: Biol. Crystallogr.* **2012**, *68* (8), 909−919.

(15) Heine, A.; Canaves, J. M.; von Delft, F.; Brinen, L. S.; Dai, X.; Deacon, A. M.; Elsliger, M. A.; Eshaghi, S.; Floyd, R.; Godzik, A.; Grittini, C.; Grzechnik, S. K.; Guda, C.; Jaroszewski, L.; Karlak, C.; Klock, H. E.; Koesema, E.; Kovarik, J. S.; Kreusch, A.; Kuhn, P.; Lesley, S. A.; McMullan, D.; McPhillips, T. M.; Miller, M. A.; Miller, M. D.; Morse, A.; Moy, K.; Ouyang, J.; Page, R.; Robb, A.; Rodrigues, K.; Schwarzenbacher, R.; Selby, T. L.; Spraggon, G.; Stevens, R. C.; van den Bedem, H.; Velasquez, J.; Vincent, J.; Wang, X.; West, B.; Wolf, G.; Hodgson, K. O.; Wooley, J.; Wilson, I. A. Crystal Structure of O-Acetylserine Sulfhydrylase (TM0665) from Thermotoga Maritima at

DOI: 10.1021/acs.jmedchem.5b01775
J. Med. Chem. XXXX, XXX, XXX−XXX

1.8 Å Resolution. *Proteins: Struct., Funct., Genet.* **2004**, *56* (2), 387−391.
(16) Claus, M. T.; Zocher, G. E.; Maier, T. H. P.; Schulz, G. E. Structure of the O-Acetylserine Sulfhydrylase Isoenzyme CysM from Escherichia Coli. *Biochemistry* **2005**, *44* (24), 8620−8626.
(17) Chattopadhyay, A.; Meier, M.; Ivaninskii, S.; Burkhard, P.; Speroni, F.; Campanini, B.; Bettati, S.; Mozzarelli, A.; Rabeh, W. M.; Li, L.; Cook, P. F. Structure, Mechanism, and Conformational Dynamics of *O* -Acetylserine Sulfhydrylase from *Salmonella Typhimurium*: Comparison of A and B Isozymes. *Biochemistry* **2007**, *46* (28), 8315−8330.
(18) Burkhard, P.; Tai, C.-H.; Jansonius, J. N.; Cook, P. F. Identification of an Allosteric Anion-Binding Site on O-Acetylserine Sulfhydrylase: Structure of the Enzyme with Chloride bound1. *J. Mol. Biol.* **2000**, *303* (2), 279−286.
(19) Jean Kumar, V. U.; Poyraz, Ö.; Saxena, S.; Schnell, R.; Yogeeswari, P.; Schneider, G.; Sriram, D. Discovery of Novel Inhibitors Targeting the Mycobacterium Tuberculosis O-Acetylserine Sulfhydrylase (CysK1) Using Virtual High-Throughput Screening. *Bioorg. Med. Chem. Lett.* **2013**, *23* (5), 1182−1186.
(20) Poyraz, Ö.; Jeankumar, V. U.; Saxena, S.; Schnell, R.; Haraldsson, M.; Yogeeswari, P.; Sriram, D.; Schneider, G. Structure-Guided Design of Novel Thiazolidine Inhibitors of O-Acetyl Serine Sulfhydrylase from Mycobacterium Tuberculosis. *J. Med. Chem.* **2013**, *56* (16), 6457−6466.
(21) Spyrakis, F.; Singh, R.; Cozzini, P.; Campanini, B.; Salsi, E.; Felici, P.; Raboni, S.; Benedetti, P.; Cruciani, G.; Kellogg, G. E.; Cook, P. F.; Mozzarelli, A. Isozyme-Specific Ligands for O-Acetylserine Sulfhydrylase, a Novel Antibiotic Target. *PLoS One* **2013**, *8* (10), e77558.
(22) Grishin, N. V.; Phillips, M. A.; Goldsmith, E. J. Modeling of the Spatial Structure of Eukaryotic Ornithine Decarboxylases. *Protein Sci.* **1995**, *4* (7), 1291−1304.
(23) Percudani, R.; Peracchi, A. The B6 Database: A Tool for the Description and Classification of Vitamin B6-Dependent Enzymatic Activities and of the Corresponding Protein Families. *BMC Bioinf.* **2009**, *10*, 273.
(24) Campanini, B.; Benoni, R.; Bettati, S.; Beck, C. M.; Hayes, C. S.; Mozzarelli, A. Moonlighting O-Acetylserine Sulfhydrylase: New Functions for an Old Protein. *Biochim. Biophys. Acta, Proteins Proteomics* **2015**, *1854* (9), 1184−1193.
(25) Ma, D. K.; Vozdek, R.; Bhatla, N.; Horvitz, H. R. CYSL-1 Interacts with the O2-Sensing Hydroxylase EGL-9 to Promote H2S-Modulated Hypoxia-Induced Behavioral Plasticity in C. Elegans. *Neuron* **2012**, *73* (5), 925−940.
(26) Tanous, C.; Soutourina, O.; Raynal, B.; Hullo, M.-F.; Mervelet, P.; Gilles, A.-M.; Noirot, P.; Danchin, A.; England, P.; Martin-Verstraete, I. The CymR Regulator in Complex with the Enzyme CysK Controls Cysteine Metabolism in Bacillus Subtilis. *J. Biol. Chem.* **2008**, *283* (51), 35551−35560.
(27) Diner, E. J.; Beck, C. M.; Webb, J. S.; Low, D. A.; Hayes, C. S. Identification of a target cell permissive factor required for contact-dependent growth inhibition (CDI). *Genes Dev.* **2012**, *26*, 515−525.
(28) Pearson, M. M.; Yep, A.; Smith, S. N.; Mobley, H. L. T. Transcriptome of Proteus Mirabilis in the Murine Urinary Tract: Virulence and Nitrogen Assimilation Gene Expressio. *Infect. Immun.* **2011**, *79* (7), 2619−2631.
(29) Wang, Q.; Frye, J. G.; McClelland, M.; Harshey, R. M. Gene Expression Patterns during Swarming in Salmonella Typhimurium: Genes Specific to Surface Growth and Putative New Motility and Pathogenicity Genes. *Mol. Microbiol.* **2004**, *52* (1), 169−187.
(30) Turnbull, A. L.; Surette, M. G. L-Cysteine Is Required for Induced Antibiotic Resistance in Actively Swarming Salmonella Enterica Serovar Typhimurium. *Microbiology* **2008**, *154* (11), 3410−3419.
(31) Turnbull, A. L.; Surette, M. G. Cysteine Biosynthesis, Oxidative Stress and Antibiotic Resistance in Salmonella Typhimurium. *Res. Microbiol.* **2010**, *161* (8), 643−650.
(32) Campanini, B.; Pieroni, M.; Raboni, S.; Bettati, S.; Benoni, R.; Pecchini, C.; Costantino, G.; Mozzarelli, A. Inhibitors of the Sulfur Assimilation Pathway in Bacterial Pathogens as Enhancers of Antibiotic Therapy. *Curr. Med. Chem.* **2014**, *22* (2), 187−213.
(33) Salsi, E.; Bayden, A. S.; Spyrakis, F.; Amadasi, A.; Campanini, B.; Bettati, S.; Dodatko, T.; Cozzini, P.; Kellogg, G. E.; Cook, P. F.; Roderick, S. L.; Mozzarelli, A. Design of O-Acetylserine Sulfhydrylase Inhibitors by Mimicking Nature. *J. Med. Chem.* **2010**, *53* (1), 345−356.
(34) Salsi, E.; Campanini, B.; Bettati, S.; Raboni, S.; Roderick, S. L.; Cook, P. F.; Mozzarelli, A. A Two-Step Process Controls the Formation of the Bienzyme Cysteine Synthase Complex. *J. Biol. Chem.* **2010**, *285* (17), 12813−12822.
(35) Zhao, C.; Moriga, Y.; Feng, B.; Kumada, Y.; Imanaka, H.; Imamura, K.; Nakanishi, K. On the Interaction Site of Serine Acetyltransferase in the Cysteine Synthase Complex from Escherichia Coli. *Biochem. Biophys. Res. Commun.* **2006**, *341* (4), 911−916.
(36) Campanini, B.; Speroni, F.; Salsi, E.; Cook, P. F.; Roderick, S. L.; Huang, B.; Bettati, S.; Mozzarelli, A. Interaction of Serine Acetyltransferase with *O* -Acetylserine Sulfhydrylase Active Site: Evidence from Fluorescence Spectroscopy. *Protein Sci.* **2005**, *14* (8), 2115−2124.
(37) Spyrakis, F.; Felici, P.; Bayden, A. S.; Salsi, E.; Miggiano, R.; Kellogg, G. E.; Cozzini, P.; Cook, P. F.; Mozzarelli, A.; Campanini, B. Fine Tuning of the Active Site Modulates Specificity in the Interaction of O-Acetylserine Sulfhydrylase Isozymes with Serine Acetyltransferase. *Biochim. Biophys. Acta, Proteins Proteomics* **2013**, *1834* (1), 169−181.
(38) Amori, L.; Katkevica, S.; Bruno, A.; Campanini, B.; Felici, P.; Mozzarelli, A.; Costantino, G. Design and Synthesis of Trans-2-Substituted-Cyclopropane-1-Carboxylic Acids as the First Non-Natural Small Molecule Inhibitors of O-Acetylserine Sulfhydrylase. *MedChemComm* **2012**, *3* (9), 1111.
(39) Bray, C. D.; Minicone, F. Stereocontrolled Synthesis of Quaternary Cyclopropyl Esters. *Chem. Commun.* **2010**, *46* (32), 5867−5869.
(40) Beato, C.; Pecchini, C.; Cocconcelli, C.; Campanini, B.; Marchetti, M.; Pieroni, M.; Mozzarelli, A.; Costantino, G. Cyclopropane Derivatives as Potential Human Serine Racemase Inhibitors: Unveiling Novel Insights into a Difficult Target. *J. Enzyme Inhib. Med. Chem.* **2016**, 1−8.
(41) Pieroni, M.; Annunziato, G.; Azzali, E.; Dessanti, P.; Mercurio, C.; Meroni, G.; Trifiró, P.; Vianello, P.; Villa, M.; Beato, C.; Varasi, M.; Costantino, G. Further Insights into the SAR of α-Substituted Cyclopropylamine Derivatives as Inhibitors of Histone Demethylase KDM1A. *Eur. J. Med. Chem.* **2015**, *92*, 377−386.
(42) Hackelöer, K.; Schnakenburg, G.; Waldvogel, S. R. Oxidative Coupling Reactions of 1,3-Diarylpropene Derivatives to Dibenzo[a,c]-cycloheptenes by PIFA. *Eur. J. Org. Chem.* **2011**, *2011* (31), 6314−6319.
(43) Özer, G.; Saraçoğlu, N.; Balci, M. Synthesis and Chemistry of Unusual Bicyclic Endoperoxides Containing the Pyridazine Ring. *J. Org. Chem.* **2003**, *68* (18), 7009−7015.
(44) Benci, S.; Bettati, S.; Vaccari, S.; Schianchi, G.; Mozzarelli, A.; Cook, P. F. Conformational Probes of O-Acetylserine Sulfhydrylase: Fluorescence of Tryptophans 50 and 161. *J. Photochem. Photobiol., B* **1999**, *48* (1), 17−26.
(45) Bettati, S.; Benci, S.; Campanini, B.; Raboni, S.; Chirico, G.; Beretta, S.; Schnackerz, K. D.; Hazlett, T. L.; Gratton, E.; Mozzarelli, A. Role of Pyridoxal 5′-Phosphate in the Structural Stabilization of O-Acetylserine Sulfhydrylase. *J. Biol. Chem.* **2000**, *275* (51), 40244−40251.
(46) Bettati, S.; Campanini, B.; Vaccari, S.; Mozzarelli, A.; Schianchi, G.; Hazlett, T. L.; Gratton, E.; Benci, S. Unfolding of Pyridoxal 5′-Phosphate-Dependent O-Acetylserine Sulfhydrylase Probed by Time-Resolved Tryptophan Fluorescence. *Biochim. Biophys. Acta, Protein Struct. Mol. Enzymol.* **2002**, *1596* (1), 47−54.
(47) Campanini, B.; Raboni, S.; Vaccari, S.; Zhang, L.; Cook, P. F.; Hazlett, T. L.; Mozzarelli, A.; Bettati, S. Surface-Exposed Tryptophan

DOI: 10.1021/acs.jmedchem.5b01775
J. Med. Chem. XXXX, XXX, XXX−XXX

Residues Are Essential for O-Acetylserine Sulfhydrylase Structure, Function, and Stability. *J. Biol. Chem.* **2003**, *278* (39), 37511−37519.
(48) Chirico, G.; Bettati, S.; Mozzarelli, A.; Chen, Y.; Müller, J. D.; Gratton, E. Molecular Heterogeneity of O-Acetylserine Sulfhydrylase by Two-Photon Excited Fluorescence Fluctuation Spectroscopy. *Biophys. J.* **2001**, *80* (4), 1973−1985.
(49) Mozzarelli, A.; Bettati, S.; Pucci, A. M.; Burkhard, P.; Cook, P. F. Catalytic Competence of O-Acetylserine Sulfhydrylase in the Crystal Probed by Polarized Absorption Microspectrophotometry. *J. Mol. Biol.* **1998**, *283* (1), 135−146.
(50) Tian, H.; Guan, R.; Salsi, E.; Campanini, B.; Bettati, S.; Kumar, V. P.; Karsten, W. E.; Mozzarelli, A.; Cook, P. F. Identification of the Structural Determinants for the Stability of Substrate and Amino-acrylate External Schiff Bases in O-Acetylserine Sulfhydrylase-A. *Biochemistry* **2010**, *49* (29), 6093−6103.
(51) Cook, P. F. α,β-Elimination Reaction of O-Acetylserine Sulfhydrylase. Is the Pyridine Ring Required? *Biochim. Biophys. Acta, Proteins Proteomics* **2003**, *1647* (1−2), 66−69.
(52) Cook, P. F.; Wedding, R. T. Initial kinetic characterization of the multienzyme complex, cysteine synthetase. *Arch. Biochem. Biophys.* **1977**, *178*, 293−302.
(53) Hara, S.; Payne, M. A.; Schnackerzj, K. D.; Cook, P. F. A rapid purification procedure and computer-assisted sulfide ion selective electrode assay for O-acetylserine sulfhydrylase from *Salmonella typhimurium*. *Protein Expression Purif.* **1990**, *1*, 70−76.
(54) Hwang, C.-C.; Woehl, E. U.; Minter, D. E.; Dunn, M. F.; Cook, P. F. Kinetic Isotope Effects as a Probe of the β-Elimination Reaction Catalyzed by O-Acetylserine Sulfhydrylase. *Biochemistry* **1996**, *35* (20), 6358−6365.
(55) Rabeh, W. M.; Mather, T.; Cook, P. F. A Three-Dimensional Homology Model of the O-Acetylserine Sulfhydrylase-B from Salmonella Typhimurium. *Protein Pept. Lett.* **2006**, *13* (1), 7−13.
(56) Schnackerz, K. D.; Cook, P. F. Resolution of Pyridoxal 5′-Phosphate fromO-Acetylserine Sulfhydrylase fromSalmonella Typhi-muriumand Reconstitution of Apoenzyme with Cofactor and Cofactor Analogues as a Probe of the Cofactor Binding Site. *Arch. Biochem. Biophys.* **1995**, *324* (1), 71−77.
(57) Schnackerz, K. D.; Tai, C.-H.; Simmons, J. W. I.; Jacobson, T. M.; Rao, G. S. J.; Cook, P. F. Identification and Spectral Characterization of the External Aldimine of the O-Acetylserine Sulfhydrylase Reaction. *Biochemistry* **1995**, *34* (38), 12152−12160.
(58) Tai, C.-H.; Nalabolu, S. R.; Simmons, J. W.; Jacobson, T. M.; Cook, P. F. Acid-Base Chemical Mechanism of O-Acetylserine Sulfhydrylases-A and -B from pH Studies. *Biochemistry* **1995**, *34* (38), 12311−12322.
(59) Woehl, E. U.; Tai, C.-H.; Dunn, M. F.; Cook, P. F. Formation of the α-Aminoacrylate Intermediate Limits the Overall Reaction Catalyzed by O-Acetylserine Sulfhydrylase. *Biochemistry* **1996**, *35* (15), 4776−4783.
(60) Amadasi, A.; Bertoldi, M.; Contestabile, R.; Bettati, S.; Cellini, B.; Luigi di Salvo, M.; Borri-Voltattorni, C.; Bossa, F.; Mozzarelli, A. Pyridoxal 5-Phosphate Enzymes as Targets for Therapeutic Agents. *Curr. Med. Chem.* **2007**, *14* (12), 1291−1324.
(61) Bruno, A.; Amori, L.; Costantino, G. Computational Insights into the Mechanism of Inhibition of OASS-A by a Small Molecule Inhibitor. *Mol. Inf.* **2013**, *32* (5−6), 447−457.
(62) Mayer, M.; Meyer, B. Characterization of ligand binding by saturation transfer difference NMR spectroscopy. *Angew. Chem., Int. Ed.* **1999**, *38* (12), 1784−1788.
(63) Angulo, J.; Nieto, P. M. STD-NMR: Application to transient interactions between biomolecules-a quantitative approach. *Eur. Biophys. J.* **2011**, *40* (12), 1357−1369.
(64) Mayer, M.; Meyer, B. Group Epitope Mapping by Saturation Transfer Difference NMR To Identify Segments of a Ligand in Direct Contact with a Protein Receptor. *J. Am. Chem. Soc.* **2001**, *123* (25), 6108−6117.
(65) Jayalakshmi, V.; Krishna, N. R. Complete Relaxation and Conformational Exchange Matrix (CORCEMA) Analysis of Inter-molecular Saturation Transfer Effects in Reversibly Forming Ligand−Receptor Complexes. *J. Magn. Reson.* **2002**, *155* (1), 106−118.
(66) Rama Krishna, N.; Jayalakshmi, V. Complete Relaxation and Conformational Exchange Matrix Analysis of STD-NMR Spectra of Ligand−receptor Complexes. *Prog. Nucl. Magn. Reson. Spectrosc.* **2006**, *49* (1), 1−25.
(67) Neal, S.; Nip, A. M.; Zhang, H.; Wishart, D. S. Rapid and Accurate Calculation of Protein 1H, 13C and 15N Chemical Shifts. *J. Biomol. NMR* **2003**, *26* (3), 215−240.

DOI: 10.1021/acs.jmedchem.5b01775
J. Med. Chem. XXXX, XXX, XXX−XXX